Short Article

Cell Metabolism

Cutaneous Na^+ Storage Strengthens the Antimicrobial Barrier Function of the Skin and Boosts Macrophage-Driven Host Defense

Graphical Abstract

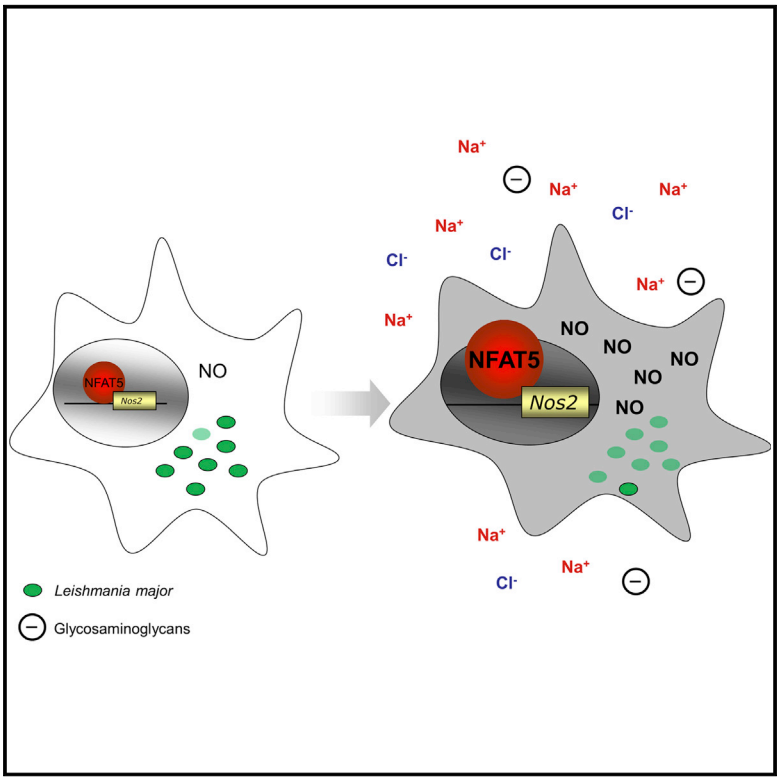

Authors

Jonathan Jantsch, Valentin Schatz, ..., Friedrich C. Luft, Jens Titze

Correspondence

Jonathan.Jantsch@ukr.de

In Brief

Jantsch et al. show that Na^+ accumulates in infected skin in humans and mice and creates a hypertonic microenvironment increasing NO production in macrophages to facilitate pathogen removal. High-salt diet promotes skin Na^+ accumulation, which boosts macrophage activation and helps resolve bacterial infection.

Highlights

- Na^+ accumulates at site of bacterial skin infections in humans and in mice
- Salt boosts classical macrophage (MΦ) activation and wards off infection
- Salt increases NOS2 activity in MΦ via p38/MAPK and NFAT5 signaling
- High-salt diet promotes skin Na^+ storage and ameliorates cutaneous leishmaniasis

Jantsch et al., 2015, Cell Metabolism *21*, 493–501
March 3, 2015
http://dx.doi.org/10.1016/j.cmet.2015.02.003

Cell Metabolism
Short Article

Cutaneous Na^+ Storage Strengthens the Antimicrobial Barrier Function of the Skin and Boosts Macrophage-Driven Host Defense

Jonathan Jantsch,[1,2,15,*] Valentin Schatz,[1,2,15] Diana Friedrich,[1,3,15] Agnes Schröder,[3] Christoph Kopp,[3] Isabel Siegert,[1] Andreas Maronna,[4] David Wendelborn,[1,3] Peter Linz,[3] Katrina J. Binger,[9,10] Matthias Gebhardt,[9,10] Matthias Heinig,[10,11] Patrick Neubert,[3] Fabian Fischer,[1] Stefan Teufel,[6,7] Jean-Pierre David,[6,7] Clemens Neufert,[8] Alexander Cavallaro,[5] Natalia Rakova,[9] Christoph Küper,[12] Franz-Xaver Beck,[12] Wolfgang Neuhofer,[13] Dominik N. Muller,[9,10] Gerold Schuler,[4] Michael Uder,[5] Christian Bogdan,[1] Friedrich C. Luft,[9,14] and Jens Titze[3,14]

[1]Microbiology Institute – Clinical Microbiology, Immunology and Hygiene, Universitätsklinikum Erlangen and Friedrich-Alexander Universität (FAU) Erlangen-Nürnberg, Erlangen, Germany
[2]Institute of Clinical Microbiology and Hygiene, Universitätsklinikum Regensburg and Universität Regensburg, Regensburg, Germany
[3]Interdisciplinary Center for Clinical Research and Department of Nephrology and Hypertension
[4]Department of Dermatology
[5]Department of Radiology
[6]Department of Internal Medicine 3, Rheumatology and Immunology
Universitätsklinikum Erlangen and Friedrich-Alexander Universität (FAU) Erlangen-Nürnberg, Germany
[7]Institute for Osteology and Biomechanics, University Medical Center Hamburg-Eppendorf, Hamburg, Germany
[8]Department of Internal Medicine 1, Universitätsklinikum Erlangen, Friedrich-Alexander-Universität Erlangen-Nürnberg
[9]Experimental and Clinical Research Center (ECRC), an institutional cooperation between the Charité Medical Faculty and the Max-Delbrück Center for Molecular Medicine, Berlin, Germany
[10]Max-Delbrück Center for Molecular Medicine, Berlin Germany
[11]Department of Computational Biology, Max Planck Institute for Molecular Genetics, Berlin, Germany
[12]Department of Physiology, Ludwig-Maximilians-Universität München, Munich, Germany
[13]V. Medical Clinic, University Hospital Mannheim, Mannheim, Germany
[14]Divison of Clinical Pharmacology, Vanderbilt University School of Medicine, Nashville, TN 37232, USA
[15]Co-first author
*Correspondence: Jonathan.Jantsch@ukr.de
http://dx.doi.org/10.1016/j.cmet.2015.02.003

SUMMARY

Immune cells regulate a hypertonic microenvironment in the skin; however, the biological advantage of increased skin Na^+ concentrations is unknown. We found that Na^+ accumulated at the site of bacterial skin infections in humans and in mice. We used the protozoan parasite *Leishmania major* as a model of skin-prone macrophage infection to test the hypothesis that skin-Na^+ storage facilitates antimicrobial host defense. Activation of macrophages in the presence of high NaCl concentrations modified epigenetic markers and enhanced p38 mitogen-activated protein kinase (p38/MAPK)-dependent nuclear factor of activated T cells 5 (NFAT5) activation. This high-salt response resulted in elevated type-2 nitric oxide synthase (*Nos2*)-dependent NO production and improved *Leishmania major* control. Finally, we found that increasing Na^+ content in the skin by a high-salt diet boosted activation of macrophages in a *Nfat5*-dependent manner and promoted cutaneous antimicrobial defense. We suggest that the hypertonic microenvironment could serve as a barrier to infection.

INTRODUCTION

The skin, the lungs, the intestine, and the kidneys are physiological regulators of internal environment composition by forming effective biological barriers that seal our body's constant *milieu intérieur* from an inconstant and hostile external environment. The skin serves as a barrier against physical and chemical assaults, such as dehydration and UV radiation (Proksch et al., 2008). It also forms an antimicrobial barrier that shapes the commensal skin microbiota and prevents invasion of microorganisms (Belkaid and Segre, 2014). The antimicrobial function of this barrier requires the production of antimicrobial peptides and lipids (Braff and Gallo, 2006; Fischer et al., 2014) and the interaction between keratinocytes and immune cells (Schröder, 2010). Experimental modification of skin barrier components culminates in mild to lethal phenotypes (Proksch et al., 2008).

Na^+ metabolism may represent an unappreciated functional component of skin barrier formation. Large amounts of Na^+ are stored in the skin. Skin Na^+ storage can be induced experimentally by dietary salt (Ivanova et al., 1978; Padtberg, 1910; Titze et al., 2004; Wahlgren, 1909). Recent advances in magnetic resonance imaging allow for non-invasive quantification of Na^+ storage in the skin in humans and revealed that cutaneous Na^+ stores increase with age (Linz et al., 2015). This age-dependent Na^+ accumulation is associated with primary (essential) and secondary hypertension (Kopp et al., 2012, 2013; Linz et al., 2015). Experimental studies suggest that Na^+ storage creates

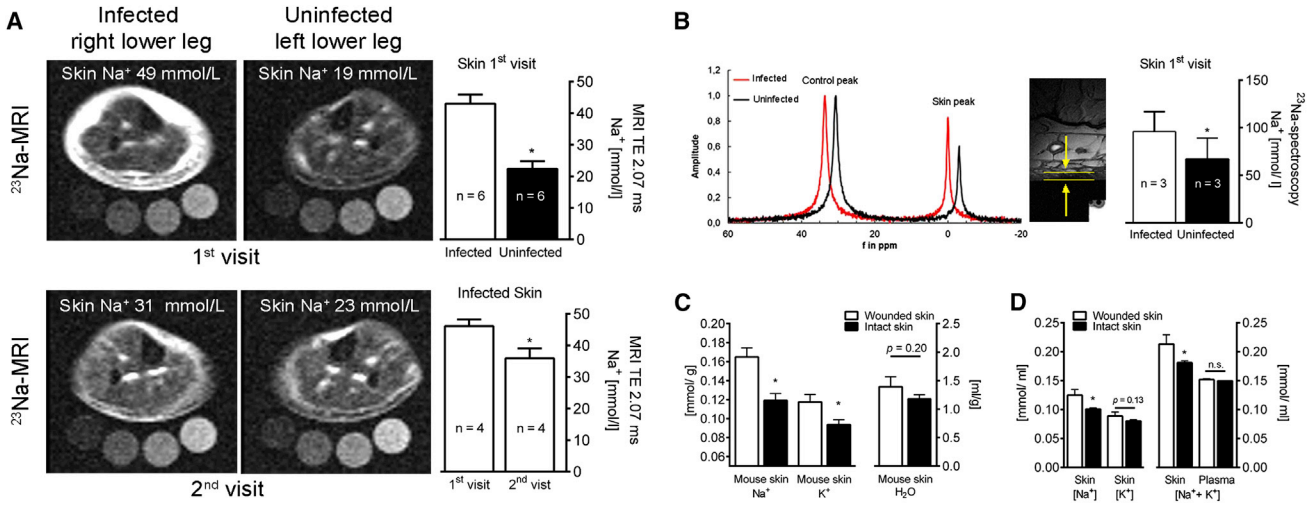

Figure 1. Infection Increases Na^+ Storage in Skin of Man and Mouse

(A) ^{23}Na MRI of an infected and contralateral uninfected lower leg with bacterial skin infection. Upper left panel, acute (1^{st}) visit; lower left panel, 28 days after antibiotics (2^{nd} visit). Upper right panel, ^{23}Na MRI estimates of 1^{st} visit (mmol/l relative to standards; mean + SEM; n = 6). Lower right panel, ^{23}Na MRI estimates (mmol/l relative to standards) of 1^{st} and 2^{nd} visit (mean + SEM; n = 4). TE: echo time in ms.

(B) Skin ^{23}Na magnetic resonance spectrogram at 1^{st} visit (skin peak). Control peak (100 mmol/l Na^+ standard with shift reagent). High-resolution ^1H image for determination of skin thickness (arrows and bars). Skin Na^+ concentrations (mean + SEM; n = 3).

(C and D) Na^+, K^+, and water distribution in plasma and skin of animals with wounded skin (mean + SEM; n ≥ 6/group; < 0.1% NaCl chow, tap water). Skin water, Na^+, and K^+ contents were measured.

(C) Na^+, K^+, and H_2O content per g dry weight.

(D) Na^+-to-water, K^+-to-water, and (Na^++K^+)-to-water ratios.

a microenvironment of hyperosmolality in the skin (Wiig et al., 2013), which is also a characteristic feature of inflamed tissue (Paling et al., 2013; Schwartz et al., 2009) and of lymphatic organs (Go et al., 2004).

Immune cells residing in such hypertonic interstitial fluid compartments polarize in response to the osmotic stress and change their function. Mediated by the osmoprotective transcription factor NFAT5, macrophages (MΦ) exert homeostatic regulatory function in the Na^+-overladen interstitium of the skin and regulate Na^+ clearance from skin Na^+ stores through cutaneous lymph vessels, which lowers systemic blood pressure (Lee et al., 2014; Machnik et al., 2009; Wiig et al., 2013). In contrast, T cells exposed to high-salt microenvironments skew into a pro-inflammatory Th17 phenotype and worsen autoimmune disease (Kleinewietfeld et al., 2013; Wu et al., 2013). High-salt diets (HSDs) also aggravated *Helicobacter pylori*-induced inflammation and carcinogenesis (Gaddy et al., 2013).

While current evidence suggests that skin Na^+ deposition is linked with disease in humans, the biological advantage of Na^+ storage is unknown. We speculate that an underlying biological principle of Na^+ metabolism is to generate hypertonic microenvironments as a protective element against outside invaders. Here we show that cutaneous Na^+ stores strengthen an immunophysiological barrier to promote immune-mediated host defense.

RESULTS

Infection Increases Na^+ Storage in Skin

We visualized skin Na^+ content in patients with bacterial skin infection by ^{23}Na magnetic resonance imaging (^{23}Na MRI). Infected areas displayed remarkable Na^+ accumulation (Figures 1A and 1B), which was reduced after antibiotic treatment (Figure 1A). ^{23}Na MRI reliably detects skin-Na^+ content but underestimates Na^+ concentrations. Additional ^{23}Na spectroscopy revealed enhanced Na^+ concentrations in infected human skin (Figure 1B), which were consistent with Na^+-to-water ratios obtained by chemical analysis in bitten mice with infected skin lesions (Figures 1C and 1D). Infected mouse skin displayed ~40 mmol/l increase in (Na^++K^+)-to-water ratio, compared to plasma levels (Figure 1D). These findings suggest that immune cells entering wounded skin are exposed to a hypertonic interstitial microenvironment. We hypothesized that Na^+ accumulation within the microenvironment facilitates antimicrobial host defense.

NaCl Boosts MΦ Activation

We first tested this hypothesis in vitro and investigated the effect of salt on lipopolysaccharide (LPS)-induced classical antimicrobial MΦ activation by analyzing NO and TNF release (Murray and Wynn, 2011). A 40 mM increase in culture medium NaCl concentration (HS) boosted LPS-triggered induction of *Nos2* on mRNA and protein level with enhanced NO release in RAW 264.7 MΦ and bone-marrow-derived MΦ (BMM) (Figure 2A). Parallel experiments with increased concentrations of the tonicity control, urea, (Table S1) neither increased *Nos2* expression nor NO release (Figure 2A). Similarly, HS augmented NO release in peritoneal MΦ (Figure S1A). In line with earlier data (Junger et al., 1994; Shapiro and Dinarello, 1997), HS boosted LPS-induced TNF secretion in MΦ (Figures S1B and S1C). HS also triggered NO release in BMM stimulated with IL-1α + TNF or IL-1β + TNF (Figure 2B). To study epigenetic modifications of the *Nos2* gene, we performed

chromatin immunoprecipitation DNA sequencing (Table S2). LPS boosted histone H3 lysine-4 trimethylation (H3K4me3) in the *Nos2* gene (Figures S1D and S1E), indicating activation of *Nos2* transcription (Angrisano et al., 2012). HS further augmented H3K4me3 at distinct regions in the *Nos2* gene (Figures S1D and S1E). We conclude that HS augments LPS-mediated and IL-1α or IL-1β + TNF-induced MΦ activation.

Salt-Driven MΦ Activation Depends on p38/MAPK

We next investigated LPS-driven signaling pathways that share HS responses (Denkert et al., 1998; Han et al., 1994; Lang et al., 2002; Shapiro and Dinarello, 1995) and that promote antimicrobial MΦ effector function (Kawai and Akira, 2010; Rauch et al., 2013). LPS treatment alone uniformly increased JNK (c-JUN N-terminal kinase)/MAPK, p44/42 (extracellular signal-regulated kinases, ERK)/MAPK phosphorylation (Figure S1F), and activation of NF-κB (Figure S1G). HS did not promote the activation of these signaling cascades and signal transducer and activator of transcription 1 (STAT1) (Figures S1F–S1H). Similarly, *Stat1* deficiency did not reduce the salt-driven boost in TNF release (Figure S1I). In contrast, HS augmented LPS-induced phosphorylation of p38/MAPK, its downstream target, and MAPK-activated protein kinase 2 (MK2) (Figure 2C) and increased TNF and NO release (Figure 2D). Pharmacological p38/MAPK blockade abolished MK2 activation (Figure 2C) and prevented the salt-driven boost in TNF release and NO production (Figure 2D). Similarly, genetic deletion of p38α prevented the salt-driven increase in NO production in LPS-stimulated MΦ (Figure 2E). The findings suggest that HS boosts proinflammatory MΦ activation via the p38/MAPK signaling cascade.

p38/MAPK Requires NFAT5 for HS-Driven Boost in MΦ Activation

p38/MAPK regulates NFAT5, which is pivotal for HS responses (Ko et al., 2002; Roth et al., 2010). We hypothesized that NaCl enhances p38/MAPK-dependent NFAT5 activation and boosts LPS-induced MΦ function. HS-induced osmotic stress increased NFAT5 protein expression with and without LPS stimulation and p38/MAPK blockade blunted this response (Figure 2F). NFAT5 binds to the promoters of osmoprotective genes (Ko et al., 2000; Lopez-Rodríguez et al., 1999; Miyakawa et al., 1999). *Nos2* is a known NFAT5 target gene (Buxadé et al., 2012). Whether or not NFAT5 is similarly involved in upregulating *Nos2* and subsequent NO production by HS is unknown. Reducing NFAT5 levels with *Nfat5*-specific siRNA impaired the boost in NO production in LPS-stimulated MΦ exposed to HS-induced osmotic stress (Figure 2G). In reverse, we found a large increase in NO production in *Nfat5*-overexpressing MΦ with LPS stimulation, even in the absence of a hypertonic microenvironment (Figure 2H). To demonstrate that NFAT5 was the downstream target of p38/MAPK, we blocked p38/MAPK in control and *Nfat5*-overexpressing MΦ. In contrast to controls, p38/MAPK inhibition did not reduce excess NO production in *Nfat5*-overexpressing MΦ (Figure 2I). We conclude that the HS microenvironment boosts MΦ activation via p38/MAPK-dependent NFAT5 signaling. While this specific HS response is independent of STAT1-mediated INF-γ signaling (Figure 2K), the resulting boost in NO production is as potent as the classical INF-γ-driven activation of NO production in MΦ (Figure 2G).

HS Promotes Leishmanicidal Activity via p38/MAPK-Dependent NFAT5 Signaling

We next tested the effect of HS on MΦ elimination of intracellular *Escherichia* (*E.*) *coli* and *Leishmania* (*L.*) *major*. Increasing the NaCl concentration in the cell culture medium by 40 mM boosted NO production in *E. coli*-infected MΦ and promoted *E.coli* removal (Figure 3A). Similarly, HS boosted *L. major* elimination in LPS-treated MΦ (Figure 3B). This leishmanicidal effect of HS in LPS-stimulated MΦ, which was characterized by increased *Nos2* mRNA expression (Figure S2A) and NO production (Figure 3B), was similar to the effect of IFN-γ co-stimulation ($p_{(\text{HS versus IFN-}\gamma)} = 0.232$). Blocking p38/MAPK inhibited HS-induced phosphorylation of MK2 (Figure S2B). This effect was paralleled by less NO production (Figure S2C) and reduced *L. major* killing in response to HS (Figure 3C). Similarly, *Nfat5*-deficient MΦ showed reduced NO production (Figures S2D and S2E) and a diminished killing efficiency when stimulated with LPS and HS (Figure 3D). Elimination of *L. major* depends on classical MΦ activation and subsequent NO production (Diefenbach et al., 1998; Liew et al., 1990; Mahnke et al., 2014). Accordingly, the killing of *L. major* was abrogated in LPS-treated *Nos2*$^{-/-}$ MΦ co-stimulated with either HS or INF-γ (Figures 3E and S2F). These findings demonstrate that HS-induced *Leishmania* killing is coordinated by p38/MAPK and NFAT5 activation, which increases *Nos2*-dependent NO production.

HSD Ameliorates Cutaneous *L. Major* Infection In Vivo

HSD leads to Na^+ accumulation in the skin. We tested the hypothesis that such diet-induced skin Na^+ storage may promote the healing of hind footpad infection with *L. major.* Within the first 20 days after infection, footpad thickness increased in mice fed either low-salt diet (LSD) or HSD (Figure 4A). LSD mice then showed a non-resolving course of infection with persistent skin lesions, whereas the footpad thickness steadily decreased in HSD mice. Improved healing was paralleled by increased $(Na^+ + K^+)/H_2O$ ratio in HSD mice (Figure 4B). This hypertonic microenvironment was accompanied by a significant reduction of *L. major* burden at the end of the experiment (2nd time point; Figure 4B). We found a tendency toward increased IFN-γ production in HSD mice, suggesting that *Leishmania*-specific T cell responses may be involved in improved host defense with HSD (Figure 4B). MΦ count was not different between the diet groups (Figure 4B). In the end of the study, HSD animals showed increased *Nfat5* mRNA levels and elevated NOS2 levels (Figure 4C). These findings suggest that HSD promotes salt storage in the skin and facilitates leishmanicidal activity by enhancing NOS2 expression, especially during resolution phase of infection. We also studied mice with myeloid-cell-specific conditional *Nfat5* gene deletion (Machnik et al., 2009; Wiig et al., 2013) to test the relative contribution of NFAT5 for salt-assisted *L. major* elimination in myeloid cells in vivo. LPS-treated BMM from *LysM*^{Cre}*Nfat5*$^{fl/fl}$ mice showed reduced NFAT5 expression and NO production when exposed to salt-induced osmotic stress (Figure S3). In vivo, myeloid-cell-specific *Nfat5* deletion reduced the HSD-driven boost in NOS2 expression in lesional MΦ (Figure 4D). HSD-control mice had significantly reduced *L. major* load in the skin (Figure 4D). HSD-*LysM*^{Cre} *Nfat5*$^{fl/fl}$ mice only showed a tendency ($p = 0.058$) toward *L. major* load reduction and tended to have higher *L. major*

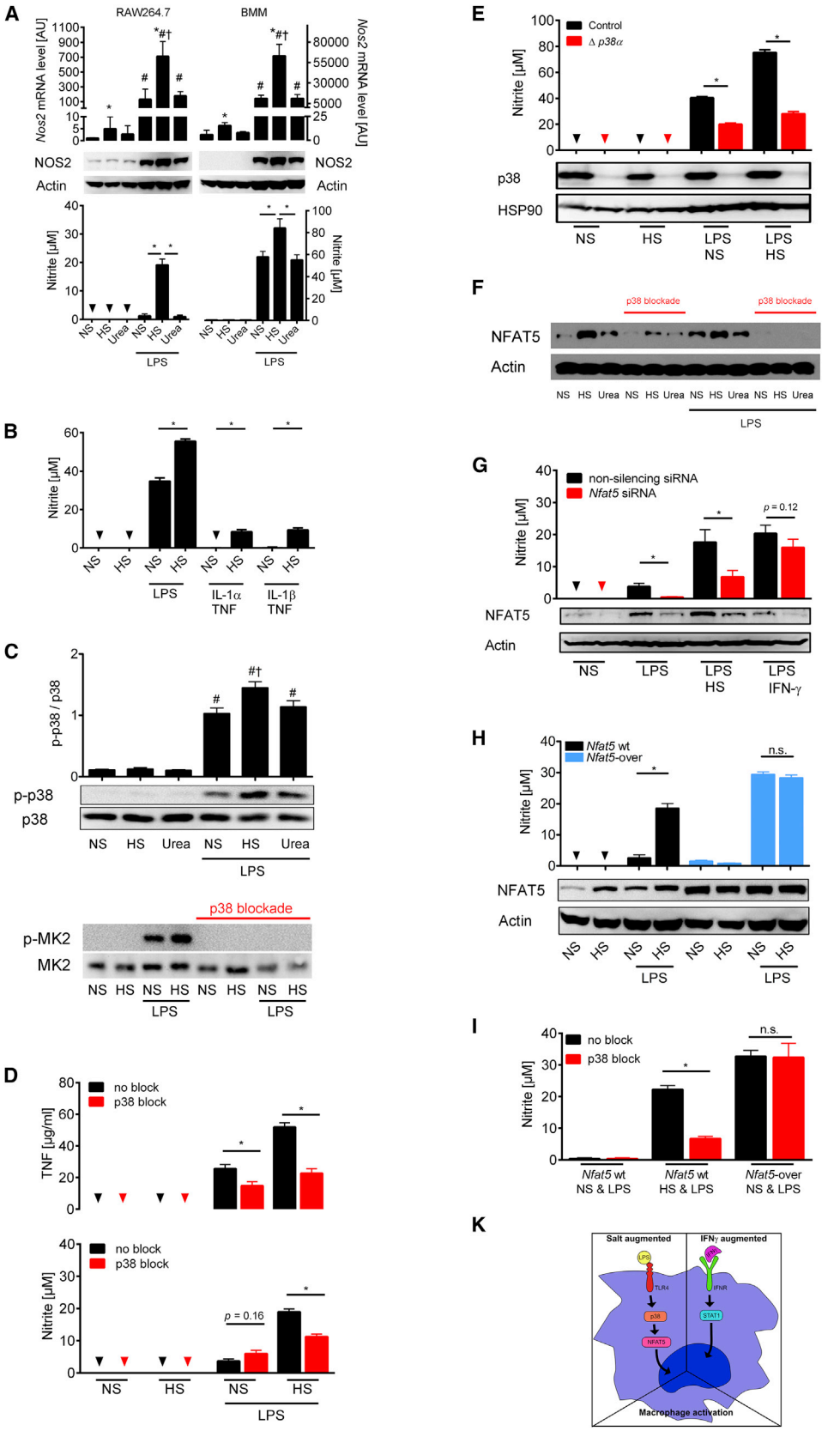

(legend on next page)

burden than controls (p = 0.078). These findings suggest *Nfat5* in myeloid cells/MΦ improves the boosting of NOS2 expression in MΦ entering the salt-overloaded microenvironment in the skin and thereby facilitates anti-leishmanial control in vivo.

DISCUSSION

We show in humans and in mice that skin-Na^+ accumulation occurs during cutaneous bacterial infections and endogenously boosts antimicrobial capacity in MΦ. Our findings support the idea that salt metabolism is a physiological component in cutaneous immunological barrier formation to ward off infections. Salt deposition might serve as an ancient mechanism to aid in immune-mediated pathogen removal.

Na^+ Storage and Skin Barrier Generation

The skin epidermis harbors a liquid-liquid interphase, where tight-junctions compartmentalize the extracellular fluid space and prevent transepidermal water losses (Furuse et al., 2002; Tunggal et al., 2005). Furthermore, active Na^+ transport by keratinocytes may create an additional physiological fluid barrier with high osmolality inside or directly under the epidermis (Hofmeister et al., 2015; Warner et al., 1988). High magnetic strength (7 Tesla) ^{23}Na MRI analyses have confirmed the existence of this Na^+-rich fluid layer in the human skin (Linz et al., 2015). Our ^{23}Na MRI measurements at 3 T underestimate the real skin Na^+ concentration, mainly due to partial volume effects arising from a mismatch of MRI resolution (3 × 3 mm) and thickness of the skin layer (1 mm). To overcome this limitation, we employed ^{23}Na spectroscopy combined with high-resolution proton imaging. Skin Na^+ concentrations obtained with this technology are of the same magnitude order as data obtained by chemical analysis of mouse skin. Our findings suggest that edema formation in infection is not only characterized by water retention and swelling but also creates a microenvironment of high Na^+ concentration. Because direct interstitial fluid collections for osmolality measurements in our patients were not possible in this non-invasive clinical ^{23}Na MRI study, additional experiments will be necessary to address the relevance of these findings to human disease.

Na^+-Enriched Skin Microenvironment Promotes Host Defense

While the mechanisms by which Na^+ is concentrated within the infected skin remain unknown, we show in mice that the osmotic stress within the Na^+-loaded interstitial fluid matrix boosts the antimicrobial host defense and thereby strengthens the anti-infectious barrier function of the skin. The increased cutaneous Na^+ concentrations in HSD mice improved *L. major* killing in the Na^+ reservoir. We conclude that dietary salt bears a therapeutic potential to promote anti-microbial barrier function of the skin.

The cure of cutaneous leishmaniasis relies on the ability of MΦ to induce *Nos2* and produce high NO levels (Mougneau et al., 2011). Our data suggest that the p38/NFAT5-dependent boost in NOS2 expression in MΦ exposed HS microenvironment in vitro and in vivo contributes to the enhanced leishmanicidal activity. In addition, salt may activate other antimicrobial effectors and pathways. Phagosomal acidification and oxidative burst are interconnected with ion fluxes (Soldati and Neyrolles, 2012) and could be sensitive to changes in interstitial Na^+ concentration. Furthermore, salt-induced enhancement of inflammatory leukocyte function is not only confined to MΦ, but also is evident in T cells (Woehrle et al., 2010). Our finding of increased *Leishmania*-specific T cell responses in HSD mice indicates an additional role of T cells in the salt-driven boost in host defense. We mechanistically focused on MΦ and the role of p38/NFAT5-driven *Nos2*-dependent NO production in the salt-driven boost of host defense. Further investigation of other cells and mechanisms involved in this microenvironment-triggered immune response is warranted in the future.

EXPERIMENTAL PROCEDURES

Tissue Electrolyte Analysis, ^{23}Na MRI, and ^{23}Na Spectroscopy of Human Skin

Chemical analysis of the carcasses included Na^+, K^+, and water measurements after dry ashing of the skin (Machnik et al., 2009). ^{23}Na MRI was done as described earlier (Kopp et al., 2012). For ^{23}Na spectroscopy, a ^{23}Na surface coil was implemented at a 3.0 T MR scanner. All animal experiments were carried out according to protocols approved by the Animal Welfare Committee of the local government (Regierung von Mittelfranken, Ansbach, Germany). We

Figure 2. High-Salt-Augmented LPS-Induced MΦ Activation Requires p38/MAPK-Dependent NFAT5 Signaling

(A) RAW 264.7 MΦ (left panel) and bone-marrow-derived MΦ (BMM, right panel) were cultured in normal cell culture medium (NS: normal salt), with additional 40 mM NaCl in the medium (HS: high salt), or 80 mM urea ± 10 ng/ml LPS for 24 hr. *Nos2* mRNA (mean + SEM; n = 4 [RAW264.7]; n = 4 to 5 [BMM]), * p(HS) < 0.05; # p(LPS) < 0.05; † p(LPS*HS) < 0.05; NOS2 protein, and nitrite levels (mean + SEM; n = 4 [RAW264.7]; n = 11 [BMM]); Triangles: not detectable (n.d.).

(B) BMM were cultured in NS, with HS ± LPS (1 ng/ml), IL-1α (50 ng/ml) or IL-1β (50 ng/ml) + TNF (20 ng/ml) for 24 hr. Nitrite levels (mean + SEM; 4 similar experiments); Triangles: n.d.

(C) RAW 264.7 MΦ were cultured in NS, with HS or 80 mM urea ± LPS (10 ng/ml) for 45 min. Upper panel, densitometry and immunoblotting of p38/MAPK and activated p-p38/MAPK (mean + SEM; n = 8). # p(LPS) < 0.05; † p(LPS*HS) < 0.05. Lower panel, immunoblotting detected the p38/MAPK substrate MK2 and activated p-MK2.

(D) RAW 264.7 MΦ were pretreated ± p38 blocker SB203580. After 0.5 hr cells were cultured in NS, with HS ± 10 ng/ml LPS for 24 hr. Upper panel, TNF levels (mean + SEM; n = 2 in triplicates); lower panel, nitrite levels (n = 7). Triangles: n.d.

(E) BMM from Poly(I:C)-treated Mx^{WT} $p38\alpha^{fl/fl}$ (control) and Mx^{Cre} $p38\alpha^{fl/fl}$ (Δ $p38\alpha$) mice were cultured in NS, with HS ± LPS (1 ng/ml) for 24 hr. Upper panel, nitrite levels (mean + SEM; n = 2 in quadruplicates); Triangles: n.d.; Lower panel, immunoblotting of p38/MAPK and HSP90.

(F) As in (D). Immunoblotting of NFAT5 and actin.

(G) RAW 264.7 MΦ electroporated with control non-silencing siRNA or *Nfat5*-specific siRNA (*Nfat5* siRNA) were cultured in NS or HS ± LPS (10 ng/ml) or LPS/IFN-γ under NS for 24 hr. Triangles, n.d. Immunoblotting of NFAT5 and Actin. Nitrite levels (mean + SEM; n = 3 to 4).

(H) RAW 264.7 wild-type MΦ (*Nfat5* wt) and RAW 264.7 MΦ with stable *Nfat5* overexpression (*Nfat5*-over) were cultured NS or HS ± LPS (10 ng/ml) for 24 hr. Immunoblotting of NFAT5 and actin. Nitrite levels (mean + SEM; n = 4).

(I) As in (D), but in addition RAW 264.7 MΦ with stable *Nfat5* overexpression (*Nfat5*-over) were used. A representative experiment in quintuplicates out of two independent experiments is displayed (mean + SEM).

(K) Schematic of HS-induced alterations in MΦ LPS signaling.

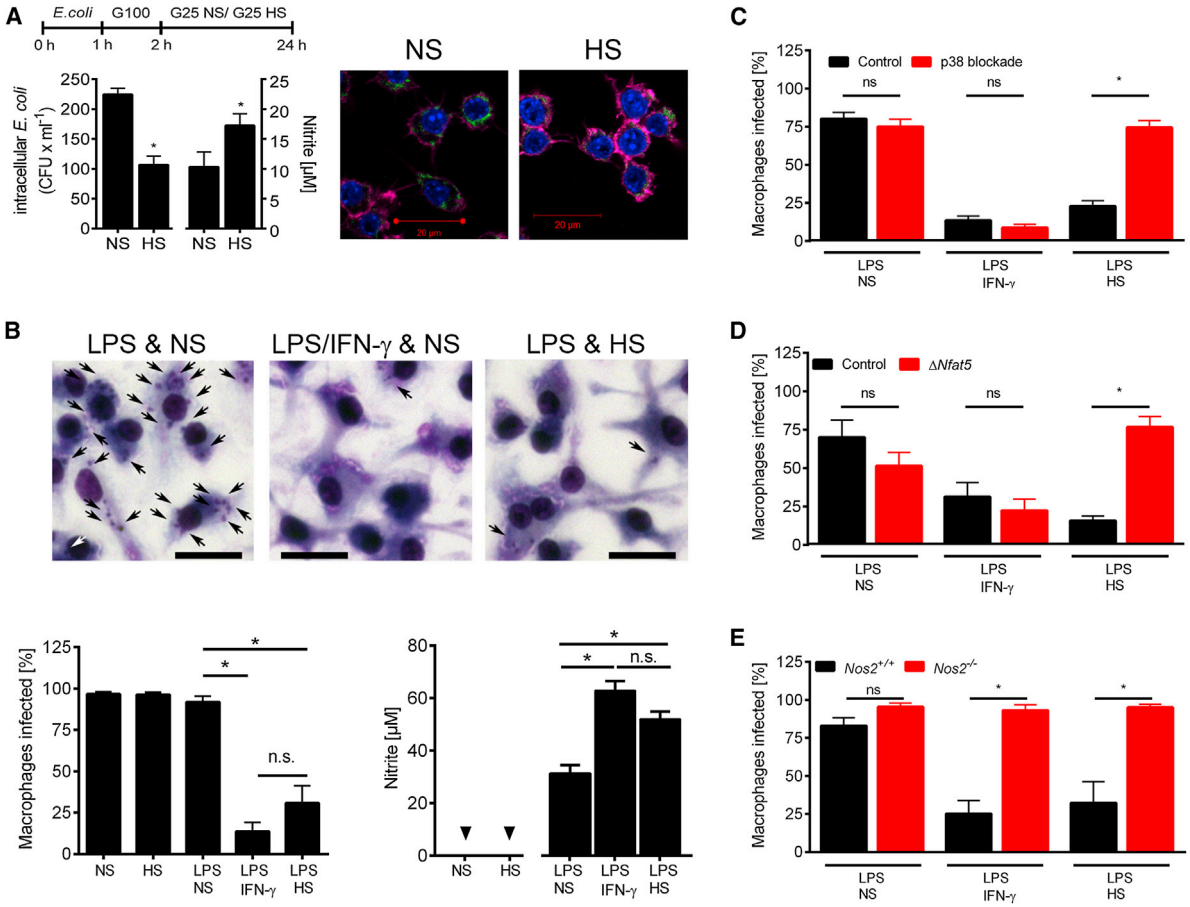

Figure 3. High-Salt Conditions Promote Anti-Microbial Activity via p38/MAPK-Dependent NFAT5 Signaling

(A) RAW 264.7 MΦ were infected with *E.coli* incubated under NS and HS conditions. Left panel, after 24 hr intracellular bacterial load and nitrite levels (mean + SEM; n = 2 at least in triplicates). Right panel, after 24 hr cells were fixed. GFP-*E.coli*, green. Phalloidin (Actin), purple. DAPI (DNA), blue. Scale bar equal 20 μm.

(B) BMM were infected with *L. major* promastigotes and stimulated with LPS (20 ng/ml) in NS or HS medium or with IFN-γ (20 ng/ml) under NS. Upper panel, Diff-Quik stains of BMM after 72 hr. Intracellular parasites, black arrows. Scale bar equals 20 μm. Lower panels, percent of infected BMM (mean + SEM; n = 5) and nitrite levels (mean + SEM; n = 7). Triangles: n.d.

(C) *L. major*-infected BMM were treated with SB203580 and stimulated as described in (A). Percent of infected BMM (mean + SEM; n = 5).

(D) As in (B), but BMM from tamoxifen-treated *Cre*-ERT2(T)^{Cre} *Nfat5*$^{fl/fl}$ (Δ*Nfat5*) and *Cre*-ERT2(T)$^{WT/WT}$ *Nfat5*$^{fl/fl}$ (control) mice were used (mean + SEM; n = 3).

(E) As in (B), but *Nos2*$^{+/+}$ and *Nos2*$^{-/-}$ BMM were used (mean + SEM; n = 3 to 4).

studied normal subjects and patients suffering from skin infection after due institutional review board approval according to the principles of the Declaration of Helsinki. Further detailed information and validation of sodium spectroscopy are in the Supplemental Experimental Procedures.

MΦ, RNAi, Immunoblotting, qPCR, and MΦ Activation and Infection Studies

Wild-type (WT) and *Nfat5*-overexpressing RAW 246.7 MΦ were used (Machnik et al., 2009). BMM were generated from C57BL/6, *Nos2*$^{-/-}$, *Stat1*$^{-/-}$, and tamoxifen-treated *Cre*-ERT2(T)^{Cre} *Nfat5*$^{fl/fl}$ and *Cre*-ERT2(T)$^{WT/WT}$ *Nfat5*$^{fl/fl}$ or Poly(I:C)-treated *Mx*^{WT} *p38α*$^{fl/fl}$ and *Mx*^{Cre} *p38α*$^{fl/fl}$ mice. RNAi, immunoblotting, and qPCR was performed as described previously (Machnik et al., 2009). Nitrite and TNF levels were assessed by Griess reaction and ELISA. BMM were infected with *L. major* promastigotes. The extracellular *L. major* were washed off, and the BMM were further cultured in the presence of the indicated stimuli for 72 hr. The percentage of infected BMM was determined microscopically. For *E. coli* infection, RAW 264.7 cells were infected with *E.coli*, and intracellular bacterial load was assessed with a gentamicin protection assay. Further detailed information is in the Supplemental Experimental Procedures.

In Vivo *L. major* Infection

After 2 weeks on LSD (<0.1% NaCl, tap water) or HSD diet (4% NaCl, 0.9% saline in the drinking water), we infected hind footpads of FVB mice and/or *LysM*^{WT} *Nfat5*$^{fl/fl}$ (control) and *LysM*^{Cre} *Nfat5*$^{fl/fl}$ mice (FVB background) with 3 × 10^6 of stationary-phase *L. major* promastigotes and continued the respective diet throughout the experiment. The number of parasites in the tissue was determined by limiting dilution analysis (Mahnke et al., 2014). Skin *Nfat5* mRNA levels and skin infiltration of CD68$^+$ MΦ was assessed as described earlier (Machnik et al., 2009). *Leishmania*-specific T cell responses were assessed by in vitro restimulation of single-cell suspensions from draining lymph nodes with soluble *Leishmania* antigens (Mahnke et al., 2014). NOS2 expression was analyzed by flow cytometry in CD11b$^+$ lesional cells. Further detailed information is in the Supplemental Experimental Procedures.

Statistical Analysis

Results are expressed as means + SEM (if not indicated otherwise). Univariate analysis using the general linear measurement procedure was used to compare data with more than one effector. Other differences were calculated by one-way ANOVA and appropriate post hoc tests or Student's t test. For non-normally distributed data, the non-parametric Mann-Whitney test was

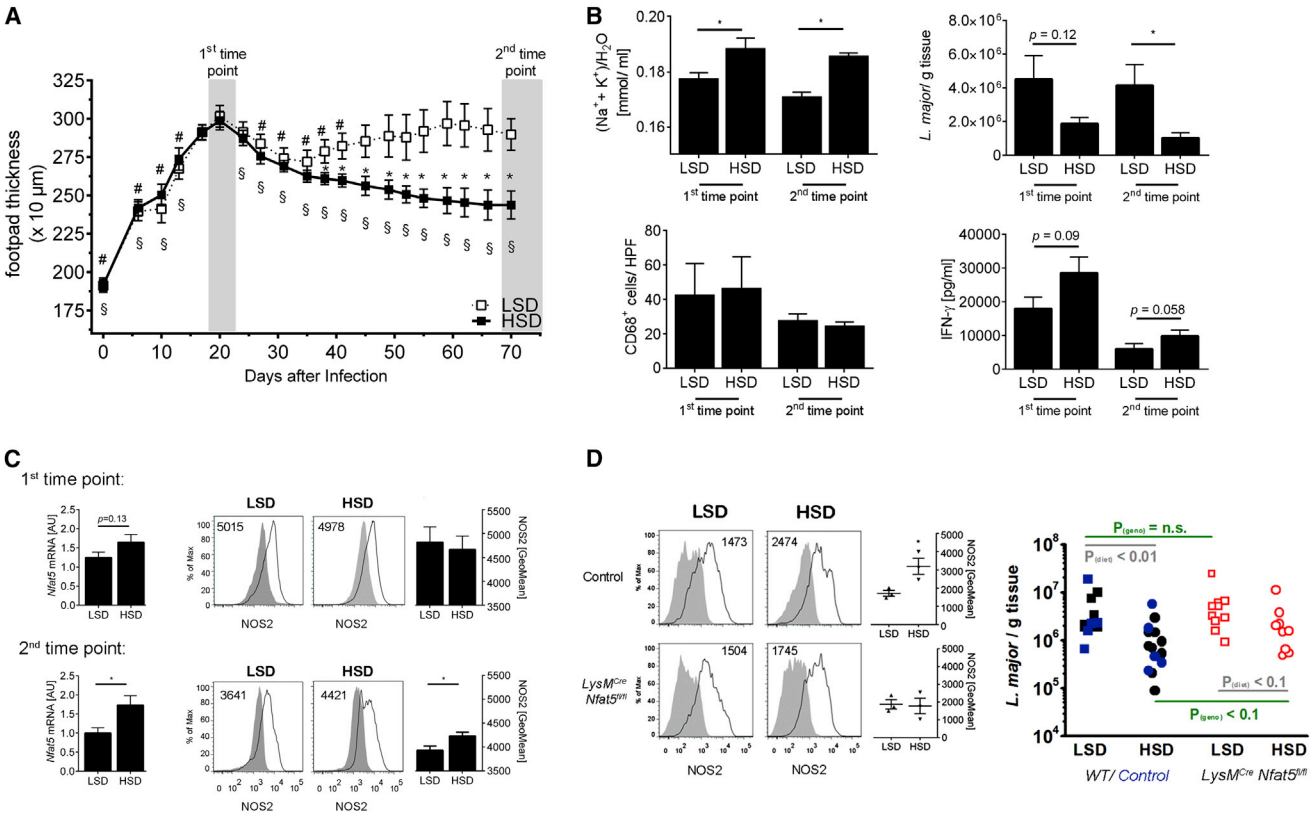

Figure 4. HSD Ameliorates *L.major* Infection In Vivo

(A–C) FVB WT mice were fed LSD or HSD throughout the experiment and infected with *L. major* promastigotes in their footpads 2 weeks after initiation of the respective diet. The diets were continued throughout the experiment.

(A) Lesion development of LSD and HSD mice (means ± 95% CI; n = 8/group). * p (versus LSD) < 0.01; # p (versus day 20 LSD) < 0.01; § p (versus day 20 HSD) < 0.01.

(B) At the 1st time point (20–24 days after infection) and at the 2nd time point (at the end of experiment), skin ($Na^+ + K^+$)-to-water ratio (mean + SEM; n ≥ 6/group); parasite burden (mean + SEM; n ≥ 7/group); amount of lesional $CD68^+$ MΦ (mean + SEM; n ≥ 3/group); and *Leishmania*-specific T cell responses (mean + SEM; n ≥ 4/group) are given.

(C) Skin *Nfat5* mRNA levels (left panel; mean + SEM; n ≥ 4) and geometric mean fluorescence of NOS2-protein expression in lesional $CD11b^+$ cells (right panel; mean + SEM; n = 4 to 5/group) at the 1st time point and at the 2nd time point. Representative histograms of NOS2 expression in lesional $CD11b^+$ cells are displayed. Insets: geometric mean fluorescence of NOS2. Grey filled area: isotype control. Black solid line: NOS2 expression.

(D) $LysM^{WT}$ $Nfat5^{fl/fl}$ (control) and $LysM^{Cre}$ $Nfat5^{fl/fl}$ were fed LSD and HSD and infected with *L. major* as described above. Left panel, as in (C) at the end of the experiment NOS2-protein expression in lesional $CD11b^+$ cells is given (mean + SEM; n = 3/group). Right panel, WT mice (black colored), $LysM^{Cre}$ $Nfat5^{fl/fl}$ (red colored), and $LysM^{WT}$ $Nfat5^{fl/fl}$ (controls, blue colored) were fed LSD or HSD and infected with *L. major* promastigotes in their footpads, as described above. Parasite burden (n = 9–14/group) in skin lesions of infected mice on a HSD or LSD for over 70 days.

used. p values of < 0.05 (*) were deemed statistically significant (if not indicated otherwise). SPPS Statistics (version 21.0, IBM) or Prism v4.0 and v6.0 (GraphPad software) were used.

ACCESSION NUMBERS

The MAGE-TAB (www.mged.org) accession number for the ChiP-Seq sequences reported in this paper is E-MTAB-3343.

SUPPLEMENTAL INFORMATION

Supplemental Information includes three figures, two tables, and Supplemental Experimental Procedures and can be found with this article online at http://dx.doi.org/10.1016/j.cmet.2015.02.003.

AUTHOR CONTRIBUTIONS

V.S., D.F., A.S., J.J., I.S., F.F., P.N., P.L., C. Kopp, D.W., S.T., K.J.B., M.G., M.H., N.R., C. Küper, D.N.M., and J.T. did experiments and analyzed the data. A.M., A.C., P.L. C. Kopp, M.U., and G.S. enrolled patients and performed MRI. C.B., C. Küper, S.T., J.P.D., C.N., F.X.B, D.N.M., K.J.B., and W.N. provided essential material and contributed to the design of the experiments. D.N.M., D.F., K.J.B., P.L., and V.S. contributed to manuscript preparation. K.J.B., D.N.M., J.J., and J.T. designed and planned the experiments and analyzed and interpreted data. J.J., C.B., F.C.L, and J.T. wrote the manuscript.

ACKNOWLEDGMENTS

The Deutsche Forschungsgemeinschaft (DFG; SFB 643 A6 and B16; DA1067/7-2) supported J.J., J.P.D., C.B., and J.T. J.T. was also supported by the German Ministry for Economics and Technology (50WB1218), the Interdisciplinary Center for Clinical Research (IZKF) Erlangen, the NIH (RO1 HL118579-01), and the American Heart Association (AHA 14SFRN20770008). C.B. was also supported by the IZKF Erlangen (A61) and the Emerging Field Initiative of the FAU. K.J.B. received an Australian National Health and Medical Research Council C.J. Martin Fellowship (APP1037633). The DFG and the German Center for Cardiovascular Research supported D.N.M. and F.C.L. We thank the

Imaging Science Institute (Erlangen) for measurement time and for technical support. We are grateful for the excellent technical assistance of Kirstin Castiglione, Andrea Debus, Heidi Sebald, Jenny Hähnel, Sabrina Cabric, Anna Birukov, Monika Nowottny, and Daniela Amslinger.

Received: June 23, 2014
Revised: December 1, 2014
Accepted: February 6, 2015
Published: March 3, 2015

REFERENCES

Angrisano, T., Lembo, F., Peluso, S., Keller, S., Chiariotti, L., and Pero, R. (2012). Helicobacter pylori regulates iNOS promoter by histone modifications in human gastric epithelial cells. Med. Microbiol. Immunol. (Berl.) *201*, 249–257.

Belkaid, Y., and Segre, J.A. (2014). Dialogue between skin microbiota and immunity. Science *346*, 954–959.

Braff, M.H., and Gallo, R.L. (2006). Antimicrobial peptides: an essential component of the skin defensive barrier. Curr. Top. Microbiol. Immunol. *306*, 91–110.

Buxadé, M., Lunazzi, G., Minguillón, J., Iborra, S., Berga-Bolaños, R., Del Val, M., Aramburu, J., and López-Rodríguez, C. (2012). Gene expression induced by Toll-like receptors in macrophages requires the transcription factor NFAT5. J. Exp. Med. *209*, 379–393.

Denkert, C., Warskulat, U., Hensel, F., and Häussinger, D. (1998). Osmolyte strategy in human monocytes and macrophages: involvement of p38MAPK in hyperosmotic induction of betaine and myoinositol transporters. Arch. Biochem. Biophys. *354*, 172–180.

Diefenbach, A., Schindler, H., Donhauser, N., Lorenz, E., Laskay, T., MacMicking, J., Röllinghoff, M., Gresser, I., and Bogdan, C. (1998). Type 1 interferon (IFNalpha/beta) and type 2 nitric oxide synthase regulate the innate immune response to a protozoan parasite. Immunity *8*, 77–87.

Fischer, C.L., Blanchette, D.R., Brogden, K.A., Dawson, D.V., Drake, D.R., Hill, J.R., and Wertz, P.W. (2014). The roles of cutaneous lipids in host defense. Biochim. Biophys. Acta *1841*, 319–322.

Furuse, M., Hata, M., Furuse, K., Yoshida, Y., Haratake, A., Sugitani, Y., Noda, T., Kubo, A., and Tsukita, S. (2002). Claudin-based tight junctions are crucial for the mammalian epidermal barrier: a lesson from claudin-1-deficient mice. J. Cell Biol. *156*, 1099–1111.

Gaddy, J.A., Radin, J.N., Loh, J.T., Zhang, F., Washington, M.K., Peek, R.M., Jr., Algood, H.M., and Cover, T.L. (2013). High dietary salt intake exacerbates Helicobacter pylori-induced gastric carcinogenesis. Infect. Immun. *81*, 2258–2267.

Go, W.Y., Liu, X., Roti, M.A., Liu, F., and Ho, S.N. (2004). NFAT5/TonEBP mutant mice define osmotic stress as a critical feature of the lymphoid microenvironment. Proc. Natl. Acad. Sci. USA *101*, 10673–10678.

Han, J., Lee, J.D., Bibbs, L., and Ulevitch, R.J. (1994). A MAP kinase targeted by endotoxin and hyperosmolarity in mammalian cells. Science *265*, 808–811.

Hofmeister, L.H., Perisic, S., and Titze, J. (2015). Tissue sodium storage: evidence for kidney-like extrarenal countercurrent systems? Pflugers Arch. *467*, 551–558.

Ivanova, L.N., Archibasova, V.K., and Shterental', I.Sh. (1978). [Sodium-depositing function of the skin in white rats]. Fiziol. Zh. SSSR Im. I M Sechenova *64*, 358–363.

Junger, W.G., Liu, F.C., Loomis, W.H., and Hoyt, D.B. (1994). Hypertonic saline enhances cellular immune function. Circ. Shock *42*, 190–196.

Kawai, T., and Akira, S. (2010). The role of pattern-recognition receptors in innate immunity: update on Toll-like receptors. Nat. Immunol. *11*, 373–384.

Kleinewietfeld, M., Manzel, A., Titze, J., Kvakan, H., Yosef, N., Linker, R.A., Muller, D.N., and Hafler, D.A. (2013). Sodium chloride drives autoimmune disease by the induction of pathogenic TH17 cells. Nature *496*, 518–522.

Ko, B.C., Turck, C.W., Lee, K.W., Yang, Y., and Chung, S.S. (2000). Purification, identification, and characterization of an osmotic response element binding protein. Biochem. Biophys. Res. Commun. *270*, 52–61.

Ko, B.C., Lam, A.K., Kapus, A., Fan, L., Chung, S.K., and Chung, S.S. (2002). Fyn and p38 signaling are both required for maximal hypertonic activation of the osmotic response element-binding protein/tonicity-responsive enhancer-binding protein (OREBP/TonEBP). J. Biol. Chem. *277*, 46085–46092.

Kopp, C., Linz, P., Wachsmuth, L., Dahlmann, A., Horbach, T., Schöfl, C., Renz, W., Santoro, D., Niendorf, T., Müller, D.N., et al. (2012). (23)Na magnetic resonance imaging of tissue sodium. Hypertension *59*, 167–172.

Kopp, C., Linz, P., Dahlmann, A., Hammon, M., Jantsch, J., Müller, D.N., Schmieder, R.E., Cavallaro, A., Eckardt, K.U., Uder, M., et al. (2013). 23Na magnetic resonance imaging-determined tissue sodium in healthy subjects and hypertensive patients. Hypertension *61*, 635–640.

Lang, K.S., Fillon, S., Schneider, D., Rammensee, H.G., and Lang, F. (2002). Stimulation of TNF alpha expression by hyperosmotic stress. Pflugers Arch. *443*, 798–803.

Lee, K.M., Danuser, R., Stein, J.V., Graham, D., Nibbs, R.J., and Graham, G.J. (2014). The chemokine receptors ACKR2 and CCR2 reciprocally regulate lymphatic vessel density. EMBO J. *33*, 2564–2580.

Liew, F.Y., Millott, S., Parkinson, C., Palmer, R.M., and Moncada, S. (1990). Macrophage killing of Leishmania parasite in vivo is mediated by nitric oxide from L-arginine. J. Immunol. *144*, 4794–4797.

Linz, P., Santoro, D., Renz, W., Rieger, J., Ruehle, A., Ruff, J., Deimling, M., Rakova, N., Muller, D.N., Luft, F.C., et al. (2015). Skin sodium measured with ^{23}Na MRI at 7.0 T. NMR Biomed. *28*, 54–62.

Lopez-Rodríguez, C., Aramburu, J., Rakeman, A.S., and Rao, A. (1999). NFAT5, a constitutively nuclear NFAT protein that does not cooperate with Fos and Jun. Proc. Natl. Acad. Sci. USA *96*, 7214–7219.

Machnik, A., Neuhofer, W., Jantsch, J., Dahlmann, A., Tammela, T., Machura, K., Park, J.K., Beck, F.X., Müller, D.N., Derer, W., et al. (2009). Macrophages regulate salt-dependent volume and blood pressure by a vascular endothelial growth factor-C-dependent buffering mechanism. Nat. Med. *15*, 545–552.

Mahnke, A., Meier, R.J., Schatz, V., Hofmann, J., Castiglione, K., Schleicher, U., Wolfbeis, O.S., Bogdan, C., and Jantsch, J. (2014). Hypoxia in Leishmania major skin lesions impairs the NO-dependent leishmanicidal activity of macrophages. J. Invest. Dermatol. *134*, 2339–2346.

Miyakawa, H., Woo, S.K., Dahl, S.C., Handler, J.S., and Kwon, H.M. (1999). Tonicity-responsive enhancer binding protein, a rel-like protein that stimulates transcription in response to hypertonicity. Proc. Natl. Acad. Sci. USA *96*, 2538–2542.

Mougneau, E., Bihl, F., and Glaichenhaus, N. (2011). Cell biology and immunology of Leishmania. Immunol. Rev. *240*, 286–296.

Murray, P.J., and Wynn, T.A. (2011). Protective and pathogenic functions of macrophage subsets. Nat. Rev. Immunol. *11*, 723–737.

Padtberg, J.H. (1910). Über die Bedeutung der Haut als Chlordepot. Arch. Exp. Path. Pharm *63*, 60–79.

Paling, D., Solanky, B.S., Riemer, F., Tozer, D.J., Wheeler-Kingshott, C.A.M., Kapoor, R., Golay, X., and Miller, D.H. (2013). Sodium accumulation is associated with disability and a progressive course in multiple sclerosis. Brain *136*, 2305–2317.

Proksch, E., Brandner, J.M., and Jensen, J.M. (2008). The skin: an indispensable barrier. Exp. Dermatol. *17*, 1063–1072.

Rauch, I., Müller, M., and Decker, T. (2013). The regulation of inflammation by interferons and their STATs. JAK-STAT *2*, e23820.

Roth, I., Leroy, V., Kwon, H.M., Martin, P.Y., Féraille, E., and Hasler, U. (2010). Osmoprotective transcription factor NFAT5/TonEBP modulates nuclear factor-kappaB activity. Mol. Biol. Cell *21*, 3459–3474.

Schröder, J.M. (2010). The role of keratinocytes in defense against infection. Curr. Opin. Infect. Dis. *23*, 106–110.

Schwartz, L., Guais, A., Pooya, M., and Abolhassani, M. (2009). Is inflammation a consequence of extracellular hyperosmolarity? J. Inflamm. (Lond.) *6*, 21.

Shapiro, L., and Dinarello, C.A. (1995). Osmotic regulation of cytokine synthesis in vitro. Proc. Natl. Acad. Sci. USA *92*, 12230–12234.

Shapiro, L., and Dinarello, C.A. (1997). Hyperosmotic stress as a stimulant for proinflammatory cytokine production. Exp. Cell Res. *231*, 354–362.

Soldati, T., and Neyrolles, O. (2012). Mycobacteria and the intraphagosomal environment: take it with a pinch of salt(s)! Traffic *13*, 1042–1052.

Titze, J., Shakibaei, M., Schafflhuber, M., Schulze-Tanzil, G., Porst, M., Schwind, K.H., Dietsch, P., and Hilgers, K.F. (2004). Glycosaminoglycan polymerization may enable osmotically inactive Na+ storage in the skin. Am. J. Physiol. Heart Circ. Physiol. *287*, H203–H208.

Tunggal, J.A., Helfrich, I., Schmitz, A., Schwarz, H., Günzel, D., Fromm, M., Kemler, R., Krieg, T., and Niessen, C.M. (2005). E-cadherin is essential for in vivo epidermal barrier function by regulating tight junctions. EMBO J. *24*, 1146–1156.

Wahlgren, V. (1909). Über die Bedeutung der Gewebe als Chlordepots. Arch. Exp. Path. Pharm. *61*, 97–112.

Warner, R.R., Myers, M.C., and Taylor, D.A. (1988). Electron probe analysis of human skin: determination of the water concentration profile. J. Invest. Dermatol. *90*, 218–224.

Wiig, H., Schröder, A., Neuhofer, W., Jantsch, J., Kopp, C., Karlsen, T.V., Boschmann, M., Goss, J., Bry, M., Rakova, N., et al. (2013). Immune cells control skin lymphatic electrolyte homeostasis and blood pressure. J. Clin. Invest. *123*, 2803–2815.

Woehrle, T., Yip, L., Manohar, M., Sumi, Y., Yao, Y., Chen, Y., and Junger, W.G. (2010). Hypertonic stress regulates T cell function via pannexin-1 hemichannels and P2X receptors. J. Leukoc. Biol. *88*, 1181–1189.

Wu, C., Yosef, N., Thalhamer, T., Zhu, C., Xiao, S., Kishi, Y., Regev, A., and Kuchroo, V.K. (2013). Induction of pathogenic TH17 cells by inducible salt-sensing kinase SGK1. Nature *496*, 513–517.